Inner-shell capture and ionization in collisions of H^+, He^{2+}, and Li^{3+} projectiles with neon and carbon

A. L. Ford* and J. F. Reading*
Physics Department, Texas A&M University, College Station, Texas 77843

R. L. Becker
Physics Division, Oak Ridge National Laboratory, Oak Ridge, Tennessee 37830

(Received 31 March 1980)

Theoretical methods used previously for H^+, He^{2+}, and C^{6+} collisions with neutral argon atoms have been applied to collisions of H^+, He^{2+}, and Li^{3+} projectiles with neon, and to collisions of H^+ with carbon targets. The energy range covered by the calculations is 0.4 to 4.0 MeV/amu for the neon target, and 0.2 to 2.0 MeV/amu for carbon. We calculate single-electron amplitudes for target K-shell ionization and target K- and L-shell, to projectile K-shell, charge transfer. These single-electron amplitudes are used, in an independent-particle model that allows for multielectron processes, to compute K-shell vacancy production cross sections $\sigma_{VK}^{\mathrm{IPM}}$, and cross sections $\sigma_{C,VK}^{\mathrm{IPM}}$ for producing a charge-transfer state of the projectile in the coincidence with a K-shell vacancy in the target. These cross sections are in reasonable agreement with the recent experiments of Rødbro *et al.* at Aarhus. In particular, the calculated, as well as the experimental, $\sigma_{C,VK}$ scale with projectile nuclear charge Z_p less strongly than the Z_p^5 of the Oppenheimer-Brinkman-Kramers (OBK) approximation. For He^{2+} and Li^{3+} projectiles at collision energies below where experimental data are available, our calculated multielectron corrections to the single-electron approximation for $\sigma_{C,VK}$ are large.

I. INTRODUCTION AND SUMMARY OF OUR THEORETICAL METHOD

In a recent series of papers we have described a coupled-channels method for calculation of inner-shell ionization and charge transfer in asymmetric ion-atom collisions.[1,2] These methods have been applied to a study of H^+, He^{2+}, and C^{6+} collisions with argon atoms, in the 1 to 12 MeV/amu energy range.[3,4] For the He^{2+} and C^{6+} projectiles, interesting Z_p scaling and multielectron process effects were predicted, but there were very limited experimental data with which to make comparisons. For this reason, and to further explore the range of collision partners, we have performed similar calculations for H^+, He^{2+}, and Li^{3+} in collision with neon, and H^+ collisions with carbon. For these collisions there are the recent experiments of Rødbro *et al.*[5] with which to make comparison.

We will now briefly outline the methods we used. For more details the reader is referred to our papers referenced above. The projectile is treated as a point charge of magnitude $Z_p e^2$ moving on a classical straight line and constant-velocity path, characterized by an impact parameter B and velocity v. The interaction between the projectile and the active target electron is $V^P(\vec{r}-\vec{R}) = -Z_p e^2/|\vec{r}-\vec{R}(t)|$, where $\vec{R}(t)$ locates the projectile on its classical path at time t. The target is assumed to remain at rest at the origin. The target electrons are treated in the Hartree-Fock independent-particle model. We thus solve for the time-dependent single-electron wave functions; the effect of the other target electrons is incorporated in the potential of interaction V_T between the active electron and the rest of the target.

Each single-electron wave function ψ_λ is expanded in a set of target-centered orbitals ψ_λ^T and projectile-centered orbitals ψ_λ^P. In the present calculations the projectile-centered part of the expansion is limited to a single term that corresponds to the 1s bound state of the projectile. Thus, the target and projectile-centered parts of the expansion are

$$\psi_\lambda^T(\vec{r},R,t) = \sum_{j=1}^{N} a_{j\lambda}(t)\chi_j^T(\vec{r},R,t) \tag{1}$$

and

$$\psi_\lambda^P(\vec{r},\vec{R},t) = b_{J\lambda}(t)\chi_J^P(\vec{r},\vec{R},t)\,, \tag{2}$$

where

$$a_{j\lambda}(t) \xrightarrow[t\to-\infty]{} \delta_{j\lambda}, \quad b_{J\lambda}(t) \xrightarrow[t\to-\infty]{} 0\,. \tag{3}$$

The single-electron Hamiltonian is written as

$$H_e = [H^T + W^P(R)] + [V^P - W^P(R)] \tag{4}$$

in the target-centered channels and as

$$H_e = [H^P + W^T(R)] + [V^T - W^T(R)] \tag{5}$$

in the projectile-centered channels. Here H^T and H^P are the one-electron Hamiltonians for potentials V^T and V^P, respectively, and $W^P(R)$ and $W^T(R)$ are distortion potentials. These distortion potentials W^P and W^T are chosen to have the same long-range forms as the potentials V^P and V^T, respectively.

The target-centered expansion functions χ_j^T are obtained by diagonalizing $(H^T + W^P)$ in a finite Hilbert space. This diagonalization yields an accurate representation of the bound (occupied) Hartree-Fock orbitals of the target, and a discrete pseudostate representation of the continuum. We have discussed elsewhere[6] the special problems that arise for asymmetric collisions from using such a discrete pseudo-state spectrum in place of the exact ionization continuum. As in our earlier argon target calculations,[4] the basis used to obtain the χ_j^T consisted of nine different radial functions for s orbitals, nine for p, and seven for d orbitals. With the angular variables included, this gives a set of $9+2\times 9+3\times 7=48$ target-centered expansion functions.

For the collisions considered here, at each value of the impact parameter, the charge-transfer probability is small. It is therefore a good approximation to neglect the projectile-centered part of ψ_λ in calculating the target excitation and ionization coefficients $a_{j\lambda}(t)$. With this approximation the variational principle

$$\delta\left\langle\psi\left|\left(-i\hbar\frac{\partial}{\partial t}+H_e\right)\right|\psi\right\rangle=0 \tag{6}$$

leads to

$$\left\langle\chi_j^T\left|\left(-i\hbar\frac{\partial}{\partial t}+H_e\right)\right|\psi_\lambda^T\right\rangle=0\,. \tag{7}$$

This equation leads to a set of coupled differential equations for the $a_{j\lambda}(t)$ that we solve by a time-development operator (U-matrix) approach. This method has been used and described in detail in our earlier papers.[4,7] As only target-centered functions are involved, solving for the $a_{j\lambda}$'s is computationally very efficient.

The charge-transfer amplitude $b_{J\lambda}(t)$ is obtained from

$$\left\langle\chi_J^P\left|\left(-i\hbar\frac{\partial}{\partial t}+H_e\right)\right|\psi_\lambda^T+\psi_\lambda^P\right\rangle=0\,, \tag{8}$$

which follows from Eq. (6). This yields the t-matrix-type expression[4]

$$\tilde{b}_{J\lambda}(t_L)=-\frac{i}{\hbar}\int_{-t_L}^{t_L}dt\exp\left(i\hbar^{-1}\int_{-t_L}^{t}dt'(V_{JJ}^T-W^T)\right)\times\langle\chi_J^P|(V^T-V_{JJ}^T)|\psi_\lambda^T\rangle\,. \tag{9}$$

Here,

$$V_{JJ}^T=\langle\chi_J^P|V^T|\chi_J^P\rangle\,. \tag{10}$$

and $\tilde{b}_{J\lambda}(t)$ is related to $b_{J\lambda}(t)$ by

$$b_{J\lambda}(t)=\tilde{b}_{J\lambda}(t)\exp\left(-i\hbar^{-1}\int_{-t_L}^{t}dt'(V_{JJ}^T-W^T)\right). \tag{11}$$

Thus

$$|b_{J\lambda}(t_L)|^2=|\tilde{b}_{J\lambda}(t_L)|^2\,, \tag{12}$$

so $\tilde{b}_{J\lambda}$ may be regarded as a transition amplitude. The amplitude $\tilde{b}_{J\lambda}$, as well as the $a_{j\lambda}$'s are independent of t_L, if t_L is taken to be large enough for the projectile-target interaction to be negligibly small for $t=\pm t_L$. In Eq. (9), $\psi_\lambda^T(t)$ is given by the above described U-matrix calculation.

We note that one formal difficulty with our method is that it is not unitary. The target excitation and ionization amplitudes a_{ij} are computed as elements of a U matrix, which is by construction unitary (except for small numerical inaccuracy). That is, $\sum_j^N|a_{j\lambda}|^2=1$ where the sum is over all N of the target-centered pseudostates used in the calculation. The charge-transfer amplitudes $b_{J\lambda}$ are computed separately from the t-matrix expression of Eq. (9); hence $\sum_{j=1}^N|a_{j\lambda}|^2+|b_{J\lambda}|^2>1$. But for the collisions considered here, and where λ refers to the target K shell, the deviations from unity are at most a few percent. Still, this formal deficiency in our method points to the need for further investigation of the accuracy of the approximation made in obtaining Eq. (7) for the $a_{j\lambda}$'s. Preliminary work on this is in progress.[8]

One type of experiment for which we wish to present theoretical results is one in which a K-shell hole is detected in coincidence with an electron being bound to the projectile. Thus, within the independent-particle model the final state of the system is specified by requiring that a projectile orbital be filled and that one of the target K-shell orbitals be empty. No specification is made of the final orbital occupations except for that of the preceding sentence; all other possibilities (multiple-vacancy production, multiple capture, etc.) are summed over. We call the cross section for producing this class of final states $\sigma_{C,VK}$. In a single-electron model, the only mechanism for producing a K-shell vacancy simultaneous with the charge-transferred state is by a target K-shell electron being captured by the projectile. We call the cross section for this direct process $\sigma_{C,VK}^{SP}$. This single-particle-model cross section is given in terms of the probability amplitudes we calculate as

$$\sigma_{C,VK}^{SP}=(1.2)(4\pi)\int_0^\infty|b_{KK}(B)|^2B\,dB\,. \tag{13}$$

Here, and in the discussion to follow, the subscripts on the a's and b's refer only to the spatial quantum numbers; the spin variable contribution to the transition amplitudes is already assumed to have been evaluated. A factor of 2 in the above accounts for the two K-shell electrons in the target, and the factor 1.2 includes approximately charge transfer into excited states of the projec-

tile.[9] In previous papers we have derived[10] and discussed[4] the independent-particle-model (IPM) formula for $\sigma_{C,vK}$,

$$\sigma_{C,vK}^{\mathrm{IPM}} = (1.2)(2\pi)\int_0^\infty \rho_K^K(B) B\, dB, \tag{14}$$

where

$$\rho_K^K = 2\left|\sum_{j=1}^{F} a_{Kj}^* b_{Kj}\right|^2 + 4\left(\sum_{j=1}^{F} |b_{Kj}|^2\right)\left(1 - \sum_{j=1}^{F} |a_{Kj}|^2\right). \tag{15}$$

The result has been independently derived by Reinhardt *et al.*[11] The difference between $\sigma_{C,vK}^{\mathrm{IPM}}$ and $\sigma_{C,vK}^{\mathrm{SP}}$ is the inclusion of many different types of multiple processes in the former. In the single-particle (SP) model, it must be the K-shell electron that is captured by the projectile. Only the b_{KK} amplitude therefore enters into the expression for $\sigma_{C,vK}^{\mathrm{SP}}$. For a multielectron target, however, there are other routes by which the desired final state can be produced. For example, the K-shell vacancy could be produced by ionization and the charge capture state produced by capture from the target L shell. On the other hand, for a multielectron target one must exclude from the counting collisions in which the K-shell electron is captured, but then in the same collision the K-shell hole is refilled by the projectile knocking an L-shell electron into the K-shell hole. All such effects are included in the independent-particle model in $\sigma_{C,vK}^{\mathrm{IPM}}$. It is also important that in $\sigma_{C,vK}^{\mathrm{IPM}}$ the Pauli exclusion principle is enforced. When all the amplitudes, except for the elastic amplitude a_{KK}, are small, then multiple processes have a small probability and the difference between $\sigma_{C,vK}^{\mathrm{IPM}}$ and $\sigma_{C,vK}^{\mathrm{SP}}$ will be small.

The cross sections $\sigma_{C,vK}^{\mathrm{IPM}}$ and $\sigma_{C,vK}^{\mathrm{SP}}$ are both defined in terms of a specific theoretical model. In the experiments with which we wish to compare, the cross section that is measured is for producing an Auger electron in coincidence with a projectile, the degree of ionization of which is reduced by one. To the extent possible, the Auger electrons counted corresponded to a target-hole state with a single K vacancy and no L vacancies. But it was found experimentally that the ratio of coincidences to singles in the Auger spectrum was, within experimental uncertainty of 20%, independent of the portion of the Auger spectrum from which electrons were collected. *If* only diagram-line Auger electrons were collected experimentally, then the proper calculation would be one where the final state is specified by saying that there is charge transfer and that the target is left with one and only one hole in the K shell, and no holes in the L shell. The fact that the experimental cross section is, however, essentially independent of Auger electron energy is consistent with small multiple-process terms in $\sigma_{C,vK}^{\mathrm{IPM}}$.

II. RESULTS

Our theoretical charge-transfer results for neon targets and H^+, He^{2+}, and Li^{3+} projectiles are given in Fig. 1, and are compared there to the experimental results of Rødbro *et al.*,[5] and to the earlier experiments of Cocke *et al.*[12] for H^+ projectiles. Both $\sigma_{C,vK}^{\mathrm{SP}}$ and $\sigma_{C,vK}^{\mathrm{IPM}}$ agree reasonably well with the experimental cross sections. The major discrepancies are that the calculated cross section is too low for He^{2+} projectiles at the lower experimental energies, and that the calculation lies above the experiment at the higher energies, for both H^+ and Li^{3+} projectiles. That our charge-transfer cross sections tend to be too large on the

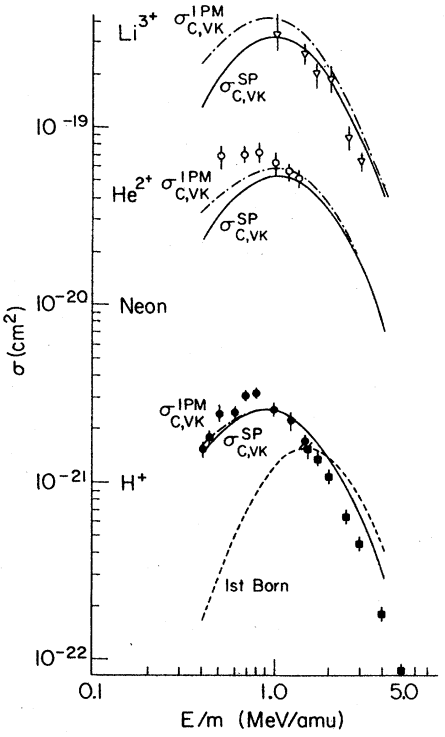

FIG. 1. Cross sections $\sigma_{C,vK}$ for producing the charge-transfer state in coincidence with a K-shell hole in the target. Cross sections for a neon target and H^+, He^{2+}, and Li^{3+} projectiles are given as a function of projectile energy E divided by the projectile mass m. The solid squares that comprise the high-energy half of the H^+ data are from Ref. 12; the other experimental points are from Ref. 5. The solid and chain curves are our theoretical results for $\sigma_{C,vK}^{\mathrm{SP}}$ and $\sigma_{C,vK}^{\mathrm{IPM}}$, respectively. The dashed curve for H^+ projectiles is the first Born result described in the text.

high-energy side of the peak has been noted previously.[3] There are a number of possible reasons for this discrepancy. A potential source of error in our calculations is our use of an independent-particle model (IPM) for the target electrons. When the electrons are captured by the projectile, they are accelerated to velocities comparable with the projectile velocity. Such electrons have sufficient energy to interact inelastically with the other target electrons. Such effects could reduce the true cross section to a value below that calculated in the IPM. The magnitude and energy dependence of the corrections to the IPM are difficult to assess theoretically, until calculations that go beyond the IPM are performed. We note that for carbon the high-energy discrepancy is small, and that for argon our calculations are uniformly too large on both sides of the cross section maximum. Another possible source of error in our calculation is lack of convergence in the number of partial waves taken in our target-centered expansion of the wave function. Assessment of this error requires further calculations that include higher angular momenta. We also point out that for p+Ne, the high-energy data (above 1.5 MeV) are from a different experiment (Ref. 12) than the low-energy data (Ref. 5). Around 1 MeV, where the experiments overlapped, there was strong disagreement in the measured variation of $\sigma_{C,VK}$ with projectile energy. The Rødbro *et al.* paper attributed this difference to an insufficiently large solid angle used in the earlier experiment, and they recommended exclusion of the two lowest-energy data points from Ref. 12 for that reason. This does not necessarily cast doubt on the high-energy data of Ref. 12, but in view of the theoretical-experimental discrepancy, an independent remeasurement of the high-energy cross section would be useful.

That $\sigma^{SP}_{C,VK}$ and $\sigma^{IPM}_{C,VK}$ differ little (compared to the size of the experimental error bars) over the energy ranges covered in the experiment is also in qualitative agreement with the experimental observations described in the previous paragraph. However, for Li^{3+} projectiles (and to a lesser extent for He^{2+}), at the lowest energies covered in the calculations there is an appreciable difference between $\sigma^{SP}_{C,VK}$ and $\sigma^{IPM}_{C,VK}$. (The difference is about a factor of 2 for Li^{3+} at 400 keV.) For this reason it would be of interest to have experimental data for Li^{3+} projectiles in the 400 to 700-keV/amu energy range.

The difference between $\sigma^{IPM}_{C,VK}$ and $\sigma^{SP}_{C,VK}$ can be decomposed into two terms,

$$\sigma^{IPM}_{C,VK} - \sigma^{SP}_{C,VK} = \delta^1_{corr} + \delta^2_{corr} , \tag{16}$$

where

$$\delta^1_{corr} = (1.2)(8\pi) \times \int_0^\infty \Big(\sum_{j=1}^{F} |b_{Kj}(B)|^2 \Big) \Big(1 - \sum_{j=1}^{F} |a_{Kj}(B)|^2 \Big) B\, dB \tag{17}$$

and

$$\delta^2_{corr} = (1.2)(4\pi) \times \int_0^\infty \Big(\Big| \sum_{j=1}^{F} a^*_{Kj}(B) b_{Kj}(B) \Big|^2 - |b_{KK}(B)|^2 \Big) B\, dB . \tag{18}$$

These two contributions to the multielectron-process corrections are given in Table I. If $\sigma^{IPM}_{C,VK}$ is to be accurately computed it is of course essential that the amplitudes that contribute to δ^1_{corr} and δ^2_{corr} be computed accurately. The δ^1_{corr} term arises from the product of the total charge-transfer probability (from all shells of the target) and the total K-shell-vacancy production probability. For these collisions the total charge capture probability is dominated by L-shell capture, particularly at the lower energies where the multielectron terms are largest. Evidence that our total charge capture probability is fairly accurate is given in Table II and also, for p+Ar collisions, in Ref. 3. The experiments being compared are both for proton projectiles. An experimental test of our computed Z_p scaling of the L-shell capture in this energy range would be valuable. The dominant con-

TABLE I. Multielectron-process terms in $\sigma^{IPM}_{C,VK}$.

Li^{3+} + Ne (Cross sections in units of 10^{-19} cm^2)				
E(MeV/amu)	$\sigma^{SP}_{C,VK}$	δ^1_{corr}	δ^2_{corr}	$\sigma^{IPM}_{C,VK}$
0.4	1.264	1.546	−0.523	2.287
0.7	2.790	1.640	−0.598	3.832
1.0	3.257	1.337	−0.499	4.095
1.5	2.728	0.710	−0.269	3.169
2.5	1.268	0.193	−0.086	1.375
4.0	0.421	0.044	−0.020	0.445
He^{2+} + Ne (Cross sections in units of 10^{-20} cm^2)				
E(MeV/amu)	$\sigma^{SP}_{C,VK}$	δ^1_{corr}	δ^2_{corr}	$\sigma^{IPM}_{C,VK}$
0.4	2.320	1.975	−0.978	3.317
0.7	4.574	1.612	−0.941	5.245
1.0	5.298	1.179	−0.590	5.887
1.5	4.554	0.571	−0.257	4.868
2.5	2.266	0.161	−0.078	2.349
4.0	0.694	0.033	−0.016	0.711
H^+ + Ne (Cross sections in units of 10^{-21} cm^2)				
E(MeV/amu)	$\sigma^{SP}_{C,VK}$	δ^1_{corr}	δ^2_{corr}	$\sigma^{IPM}_{C,VK}$
0.4	1.412	0.614	−0.441	1.585
0.7	2.354	0.321	−0.310	2.365
1.0	2.426	0.167	−0.159	2.434
1.5	1.953	0.068	−0.055	1.966
2.5	0.888	0.017	−0.010	0.895
4.0	0.284	0.004	−0.002	0.286

TABLE II. Cross-section ratio $\sigma_{C,VK}/\sigma_{CT}$, for H^+ +neon.

E/m (MeV/amu)	Expt.[a]	This calc.
1.5	13	13
2.5	34	39
4.0	55	63

[a] From Ref. 12.

tribution to the K-shell-vacancy production probability is ionization, but for the lower energies, K-shell charge transfer contributes appreciably as well. Our K-shell-vacancy production cross sections will be compared to experiment in Fig. 5. As Table I shows, the relative phases among the amplitudes are such that $\delta^2_{\rm corr}$ is negative, and this makes the total correction much smaller than $\delta^1_{\rm corr}$ alone. The target excitation and ionization and charge-transfer amplitudes that enter into $\delta^2_{\rm corr}$ are the same as in $\delta^1_{\rm corr}$. The dominant term in the integral for $\delta^2_{\rm corr}$ is $-2\,\mathrm{Re}[a_{11}b^*_{KK}(\sum_{j=2}^{F} a^*_{Kj}b_{Kj})]$, where the sum is over the L shell of neon.

It may be that our evaluation of $\sigma^{\rm IPM}_{C,VK} - \sigma^{\rm SP}_{C,VK}$ is not accurate. It is precisely to test this point that we call for further low-energy high-Z_p coincidence experiments. But regardless of whether our specific amplitudes are accurate, there is a difference in the expression for $\sigma_{C,VK}$ in the SP and IPM approximations. As the charge of the projectile is increased, and its velocity lowered, the amplitudes that enter into the correction terms of Eqs. (17) and (18) increase. It is difficult to see how the sum of $\delta^1_{\rm corr}$ and $\delta^2_{\rm corr}$ could be in all cases small if the individual amplitudes are large. Therefore, one cannot ignore the difference between $\sigma^{\rm IPM}_{C,VK}$ and $\sigma^{\rm SP}_{C,VK}$, and evaluation of the $\sigma^{\rm IPM}_{C,VK}$ is required of any complete theoretical treatment of these collisions.

In the Rødbro *et al.* paper comparison is made between the experiment and various theoretical results. We do not reproduce that comparison here; the interested reader is referred to the Rødbro *et al.* paper. All previous calculations have been for $\sigma^{\rm SP}_{C,VK}$ only. Taking the neon target data as a whole, our present theoretical results are in better agreement with the experimental cross section than are those of any previous theory. In particular, the two-state two-center calculations of Lin, while agreeing reasonably well with our calculation and with experiment for He^{2+} and Li^{3+} projectiles, fall significantly below the experiment for H^+ projectiles at 1 MeV and below.

Also shown in Fig. 1 is our first Born $\sigma^{\rm SP}_{C,VK}$ result for H^+ projectiles. For the other two projectiles the first Born $\sigma^{\rm SP}_{C,VK}$ bears a similar relation to the coupled-channels $\sigma^{\rm SP}_{C,VK}$. By first Born we mean the replacement of ψ^T_λ in Eq. (9) by the target K-shell orbital χ^T_K. It is seen that the coupled-channels corrections to this first Born approximation are quite large for these collisions.

The authors of the Rødbro *et al.* paper noted a projectile charge Z_p dependence of the cross sections somewhat less strong that the Z_p^5 of the Oppenheimer-Brinkman-Kramers (OBK).[9] The same feature is exhibited by our theoretical cross sections. This is illustrated in Fig. 2, where in 2(a) we plot $\sigma^{\rm SP}_{C,VK}/Z_p^5$ and in 2(b) we plot $\sigma^{\rm IPM}_{C,VK}/Z_p^5$, for H^+, He^{2+}, and Li^{3+}. In each figure the experimental cross section divided by Z_p^5 is also shown.

In Fig. 3 we show $\sigma^{\rm IPM}_{C,VK}$ theoretical cross sections for H^+ collisions with carbon-atom targets. On the scale of the figure the $\sigma^{\rm SP}_{C,VK}$ cross sections are indistinguishable from the $\sigma^{\rm IPM}_{C,VK}$. The experimental results given, again from Rødbro *et al.*, are for a CH_4 target. The agreement between theory and experiment is again quite good; the primary difference is that the experimental cross section lies somewhat below our theoretical prediction at the higher energies. For carbon the Hartree-Fock[13] K-shell ionization energy I_K differs by 8% from the experimental value[14] as measured, for example, in a photoelectron of x-ray experiment. This difference is due primarily to the unrelaxed final state implied in the HF calculation.[15] Which K-shell binding energy is the more correct one to use in a calculation such as ours depends on the details of the electron-ejection process, and on its time scale compared to the time scale for orbital relaxation in the target-hole state. To illustrate the magnitude of the effect on the charge-transfer cross sections introduced by this uncertainty in binding energies, in addition to calculations with HF orbital energies, we have performed calculations where the carbon K-shell energy is shifted (upward) to give agreement with the experimental I_K. The results from such a calculation are shown in Fig. 3 as triangles. There is a noticeable, but not pronounced, effect. A similar shifting of the neon K-shell orbital energy has an even smaller effect, as the fractional energy shift in that case is somewhat smaller (3%).

From the $a_{j\lambda}(t)$ amplitudes that we calculate in obtaining ψ^T_λ, we have target K-shell ionization cross sections $\sigma_{I,VK}$. In particular, in the single-particle model,

$$\sigma^{\rm SP}_{I,VK} = 2\pi \int_0^\infty \rho_K(B) B\, dB\,, \tag{19}$$

where

$$\rho_K(B) = 2\left(1 - \sum_{j=1}^{F} |a_{Kj}|^2\right). \tag{20}$$

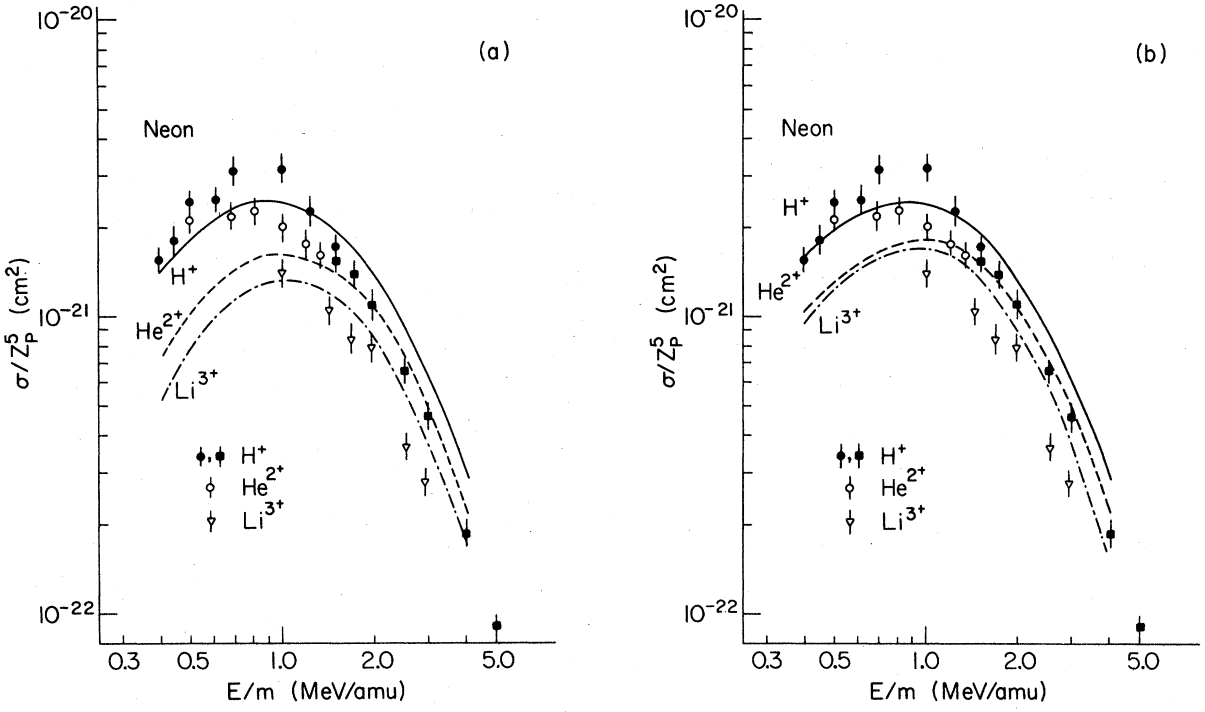

FIG. 2. The Z_p dependence of the coincidence cross section $\sigma_{C,VK}$. The cross sections presented are those of Fig. 1 divided by Z_p^5, where Z_p is the projectile charge. The theoretical cross sections in (a) are $\sigma^{SP}_{C,VK}$ and in (b) are $\sigma^{IPM}_{C,VK}$.

Here the sum is over all the initially occupied orbitals in the target. A factor of 2 in the formula appears because of the presence of two K-shell electrons. That we obtain in a single calculation, both ionization and charge-transfer amplitudes, we feel is an important feature of our method. Calculating many transition amplitudes at once is what makes it possible for us to calculate $\sigma^{IPM}_{C,VK}$

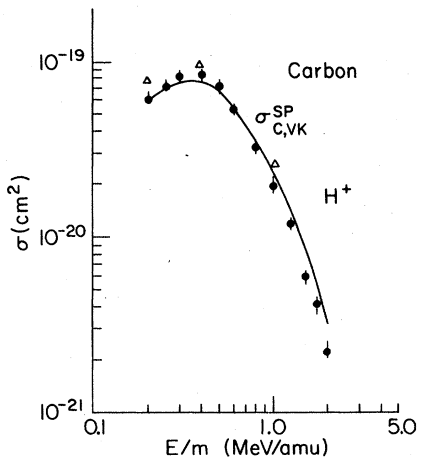

FIG. 3. Charge-transfer–K-shell hole coincidence cross sections $\sigma_{C,VK}$ as in Fig. 1, but for H^+ projectiles and a carbon-atom target. The experimental points are from Ref. 5. The theoretical curve is $\sigma^{SP}_{C,VK}$; the difference between $\sigma^{SP}_{C,VK}$ and $\sigma^{IPM}_{C,VK}$ is virtually indistinguishable on the scale of the figures. The open triangles are theoretical points calculated with the K-shell orbital energy shifted to give the experimental K-shell binding energy as described in the text.

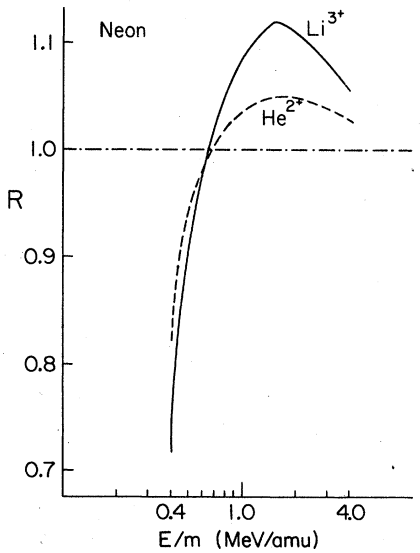

FIG. 4. The ratio $R=\sigma^{SP}_{I,VK}(Z_p)/[Z_p^2\sigma^{SP}_{I,VK}(Z_p=1)]$ for He^{2+} (dashed curve) and Li^{3+} (solid curve) projectiles on neon. Here $\sigma^{SP}_{I,VK}(Z_p)$ is our theoretical neon K-shell ionization cross section for a projectile of charge Z_p. The horizontal line at $R=1$ is the first Born prediction.

with the same ease as $\sigma^{SP}_{C,VK}$. For these collisions our K-shell ionization cross sections exhibit the well-known "increased binding" and "polarization" effects.[16,1] This is illustrated in Fig. 4, where the ratio $R = \sigma^{SP}_{I,VK}(Z_p)/[Z_p^2 \sigma^{SP}_{I,VK}(Z_p = 1)]$ is plotted for $Z_p = 2$ and 3. For the collisions studied in the present paper, there are deviations of up to 30% from the first Born prediction of $R = 1$.

In addition to the charge-transfer–K-shell-vacancy production coincidence measurements, the

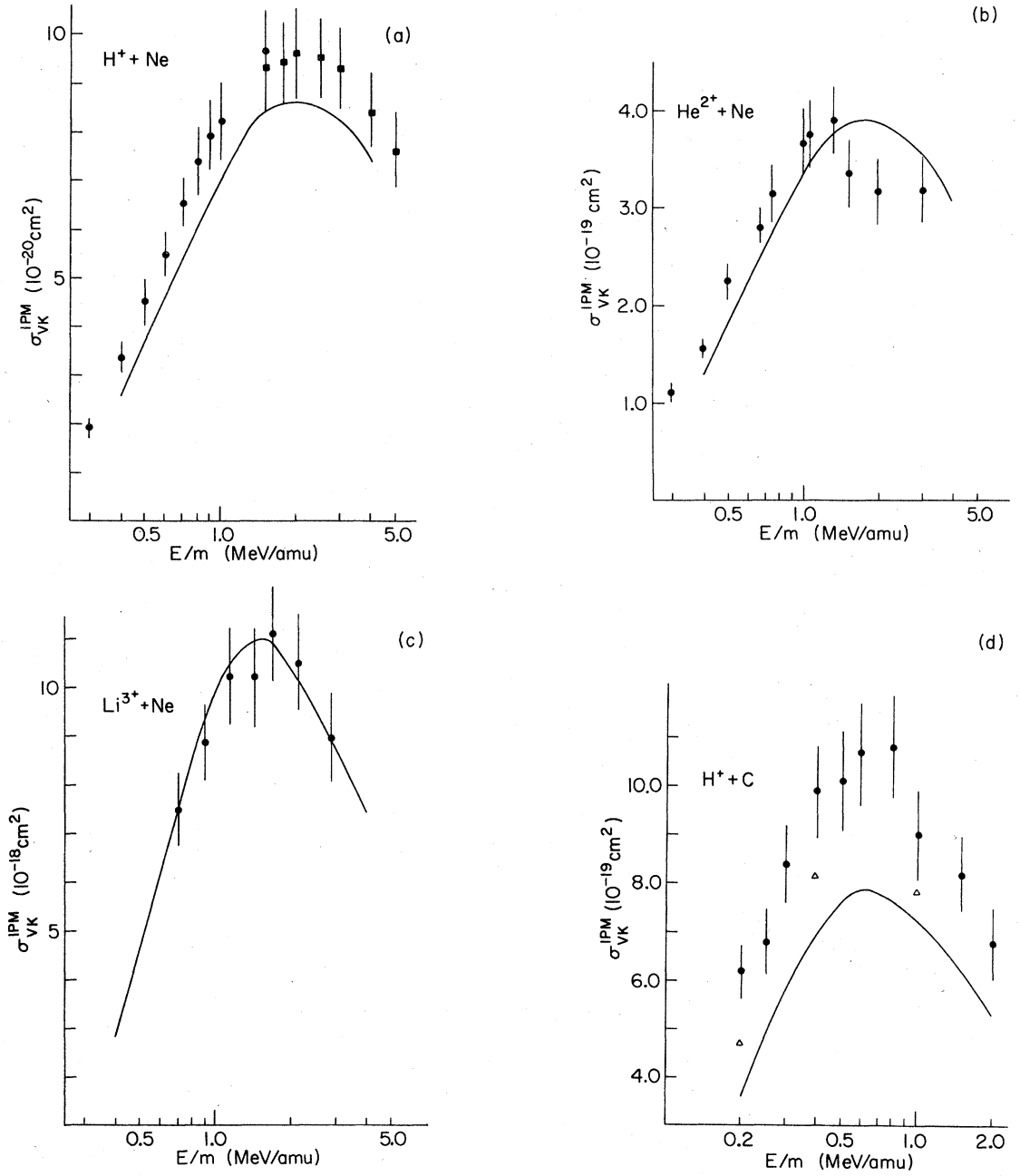

FIG. 5. K-shell-vacancy production cross sections. The solid curve in each figure is our theoretical result. The experimental points are from Ref. 5, except for the solid squares in (a), which are from Ref. 12. The experimental error bars correspond to the 10% statistical uncertainty assigned in Ref. 5. The projectile-target combinations are (a) $H^+ + Ne$, (b) $He^{2+} + Ne$, (c) $Li^{3+} + Ne$, and (d) $H^+ + C$. The open triangles in (d) are results calculated with the carbon K-shell orbital energy adjusted to give the experimental K-shell binding energy. Note that the scale on the vertical axis is linear.

Rødbro *et al.* experiment also measured K-shell-vacancy production cross sections. Our earlier paper[10] has shown that in the independent-particle model the K-shell-vacancy production cross section is given by

$$\sigma_{VK}^{\mathrm{IPM}} = \sigma_{I,VK}^{\mathrm{SP}} + \sigma_{C,VK}^{\mathrm{SP}} . \tag{21}$$

The cross section $\sigma_{VK}^{\mathrm{IPM}}$ is for producing a K-shell hole in the target, without regard to what other orbitals may or may not be occupied in the final state. Also, those final states in which there are two K-shell holes are counted twice.[10] The expression in Eq. (21) is identical to that obtained in the single-electron model ($\sigma_{VK}^{\mathrm{SP}} = \sigma_{VK}^{\mathrm{IPM}}$); the significance of this is that for this cross section all multiple-process contributions cancel in the independent-particle model. Note in particular that within the independent-particle model the charge-transfer contribution to vacancy production $\sigma_{C,VK}^{\mathrm{SP}}$ is not the same cross section as would be measured in a coincidence experiment that measures $\sigma_{C,VK}$. The experimental values[5] of σ_{VK} are compared to our calculations in Fig. 5, with the ex-

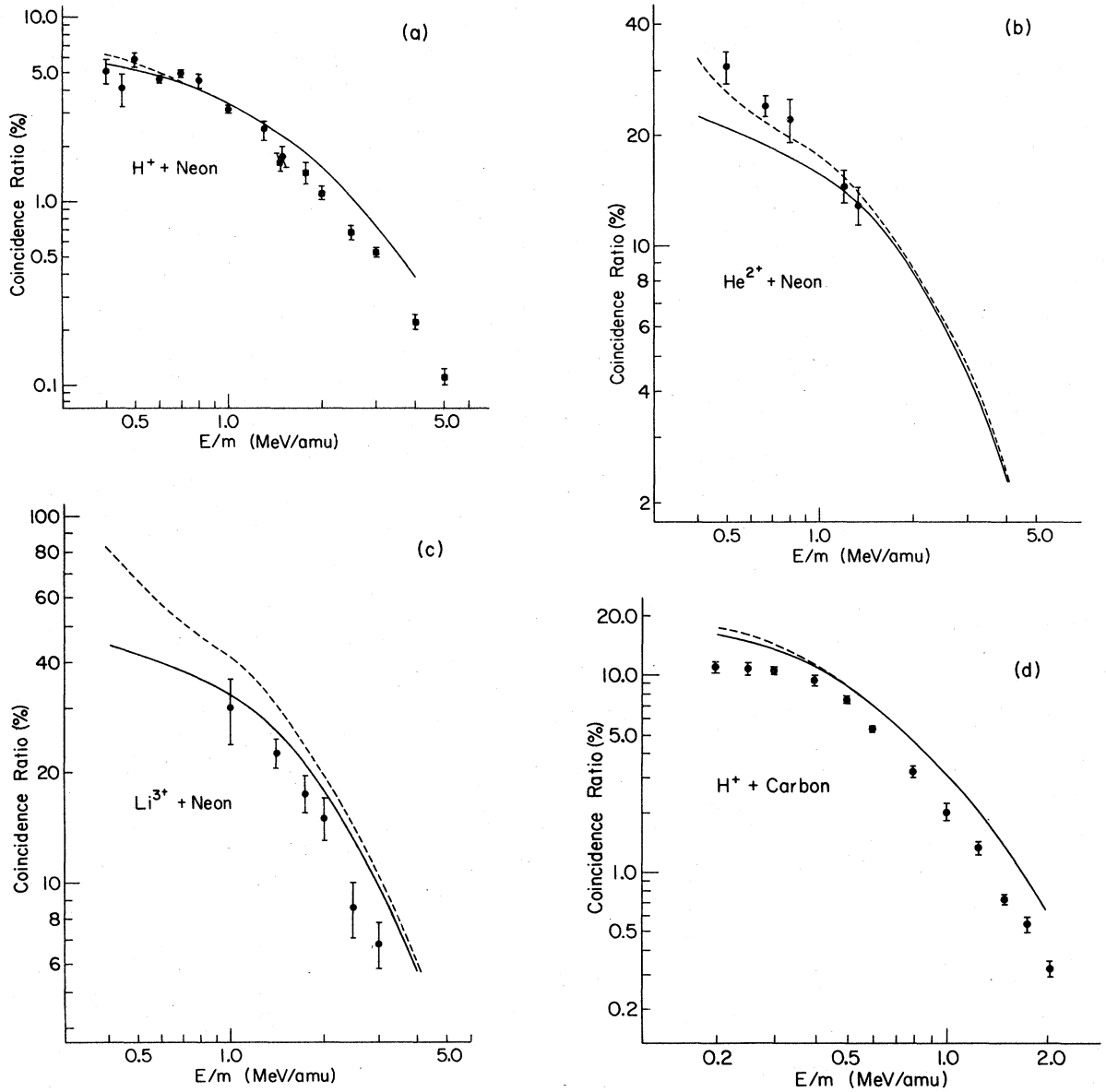

FIG. 6. Ratio between charge-transfer–K-Auger coincidences and K-Auger singles. The experimental points are from Ref. 5, except for the solid squares in (a), which are from Ref. 12. The solid curves are our calculated $\sigma_{C,VK}^{\mathrm{SP}}/\sigma_{VK}^{\mathrm{IPM}}$ cross section ratios, the dashed curves our $\sigma_{C,VK}^{\mathrm{IPM}}/\sigma_{VK}^{\mathrm{IPM}}$.

perimental uncertainty taken to be the ±10% stated in the Rødbro *et al.* paper. This uncertainty is in addition to any possible error in determining the absolute normalization. The agreement is only fair; it would appear that, compared to experiment, our K-shell ionization cross sections are in general somewhat small, and our charge-transfer cross sections too large. Another way to illustrate this, and another way to view the comparison between theory and experiment, is to look at the ratio $\sigma^{SP}_{C,vK}/\sigma^{IPM}_{vK}$ (or $\sigma^{IPM}_{C,vK}/\sigma^{IPM}_{vK}$). This ratio is measured directly in the experiment, in terms of the ratio R/A between coincidences R and single Auger electrons A. Note also that the plotted theoretical ratios $\sigma^{SP}_{C,vK}/\sigma^{IPM}_{vK}$ give one a direct picture of the projectile energy and charge dependence of the percentage contribution of charge transfer to K-shell-vacancy production. This percentage reaches as much as 40%, for 400-keV/amu Li^{3+} on neon. The comparison between theory and experiment for these ratios is made in Fig. 6. Our theoretical ratio is generally somewhat larger than the experimental one, particularly for the higher-energy collisions. This again says that our charge transfer is too large, and our ionization too small compared to the experiment. The earlier Cocke *et al.* experiment[12] also measured the ratio $\sigma_{C,vK}/\sigma_{CT}$, for H^++Ne collisions. (For the collisions they studied, our calculations give very little difference between $\sigma^{SP}_{C,vK}$ and $\sigma^{IPM}_{C,vK}$.) Here σ_{CT} is the cross section for total capture from all shells of the target $\sigma_{CT}=\sigma_{CK}+\sigma_{CL}$. For these collisions the neon L shell dominates. In our calculation σ_{CT} is obtained with very little effort beyond that required for K-shell capture. Our results are compared to the experiment in Table II; the agreement is good.

In summary, we have presented theoretical charge transfer and K-shell-vacancy production cross sections for collisions of H^+, He^{2+}, and Li^{3+} projectiles with neon, and for H^+ with carbon. These results, along with those presented earlier for H^+, He^{2+}, and C^{6+} projectiles with argon targets, provide a set of asymmetric collision cross sections that test our theoretical methods in their present stage of development. Taking all of the experimental-theoretical comparisons as a whole, the overall agreement is quite good. Our charge-transfer cross sections do appear to be too large at high energies, and our K-shell-vacancy production cross sections for H^+ projectiles tend to be somewhat too small. For the charge-transfer–K-shell-vacancy coincidence cross sections we find some cases where the independent-particle-model cross sections differ substantially from the single-particle-model results, due to multielectron-process contributions. However, these cases fall outside the energy range of the Rødbro *et al.* experiments. We urge that the coincidence experiments be done for 400 to 700-keV/amu Li^{3+} projectiles on neon to test these predictions.

ACKNOWLEDGMENTS

This research was supported by the Office of Naval Research and by the Center for Energy and Mineral Resources, Texas A&M University. At Oak Ridge the research was sponsored by the Division of Basic Energy Sciences, U. S. Department of Energy, under Contract No. W-7405-eng-26 with the Union Carbide Corporation.

*Research Participants, Physics Division, Oak Ridge National Laboratory, Oak Ridge, Tennessee 37830.

[1]J. F. Reading, A. L. Ford, and E. Fitchard, Phys. Rev. Lett. 36, 573 (1976); A. L. Ford, E. Fitchard, and J. F. Reading, Phys. Rev. A 16, 133 (1977).

[2]J. F. Reading, A. L. Ford, G. L. Swafford, and A. Fitchard, Phys. Rev. A 20, 130 (1979).

[3]A. L. Ford, J. F. Reading, and R. L. Becker, J. Phys. B 12, 2905 (1979); A. L. Ford, R. L. Becker, G. L. Swafford, and J. F. Reading, *ibid.* 12, L491 (1979).

[4]R. L. Becker, A. L. Ford, and J. F. Reading, J. Phys. B 13, 4059 (1980).

[5]M. Rødbro, E. Horsdal Pedersen, C. L. Cocke, and J. R. Macdonald, Phys. Rev. A 19, 1936 (1979).

[6]J. F. Reading and A. L. Ford, J. Phys. B 12, 1367 (1979).

[7]E. Fitchard, A. L. Ford, and J. F. Reading, Phys. Rev. A 16, 1325 (1977).

[8]J. F. Reading, A. L. Ford, and R. L. Becker (unpublished).

[9]M. R. C. McDowell and J. P. Coleman, *Introduction to the Theory of Ion-Atom Collisions* (North-Holland, Amsterdam, 1970).

[10]J. F. Reading and A. L. Ford, Phys. Rev. A 21, 124 (1980); J. F. Reading, *ibid.* 8, 3262 (1973).

[11]J. Reinhardt, B. Müller, W. Greiner, and G. Soff, Phys. Rev. Lett. 43, 1307 (1979).

[12]C. L. Cocke, R. K. Gardner, B. Curnutte, T. Bratton, and T. K. Saylor, Phys. Rev. A 16, 2248 (1977).

[13]E. Clementi and C. Roetti, At. Data Nucl. Data Tables 14, 177 (1974).

[14]J. A. Bearden and A. F. Burr, Rev. Mod. Phys. 39, 125 (1967).

[15]R. Manne and T. Aberg, Chem. Phys. Lett. 7, 282 (1970).

[16]G. Basbas, W. Brandt, R. Laubert, A. Ratkowski, and A. Schwarzchild, Phys. Rev. Lett. 27, 171 (1971); G. Basbas, W. Brandt, and R. Laubert, Phys. Rev. A 7, 983 (1974).